BENEFICIAL EFFECTS OF DOPANT COMPENSATION ON CARRIER LIFETIME IN UPGRADED METALLURGICAL SILICON

S. Dubois[1], N. Enjalbert[1], F. Servant[1], J. P. Garandet[1], R. Monna[1], J. Kraiem[2]
[1]CEA-INES, 73377 Le Bourget du Lac, France sebastien.dubois2@cea.fr
[2]Apollon Solar, 69002 Lyon, France

ABSTRACT: This study is devoted to the variations of the carrier lifetime and minority carrier diffusion length with the compensation level in solar-grade crystalline silicon. Especially we show, by using the Shockley-Read-Hall statistics, that an increase in the compensation level reduces the recombination strength of doping species and of some metal impurities. These theoretical results are confirmed by the chemical and electrical characterizations of strongly compensated multicrystalline silicon wafers and solar cells, from silicon purified by the metallurgical route. These results are of paramount importance since an accurate control of the compensation level can lead to strong improvements in silicon solar cells efficiencies. Nevertheless, possible limits of too high compensation levels are also evoked.

1 INTRODUCTION

New Solar Grade (SoG) silicon production techniques, by metallurgical route, are generally less effective in removing doping species, especially boron (B) and phosphorus (P), than the conventional Siemens process. Furthermore the use of compensated silicon for solar cell production could enlarge the choice of available feedstock and thus support the strong growth of the solar cell production capacities Hence, studies concerned with the influence of dopant compensation on the conversion efficiency of the solar cells have to be undertaken.

In the last decades, few studies were devoted to the effects of compensation on the performances of silicon solar cells. Compensation, by increasing the number of scattering centers could directly affect the mobility (μ) of both majority and minority carriers in silicon [1]. In addition compensation could be a significant source of recombination in silicon [2]. Consequently low minority carrier diffusion lengths (L), are expected to be found in compensated silicon. In contrast with what it has been previously suggested, we will show, from simulations and experimental results, that increases in the compensation level can also result in strong increases in the carrier lifetime (τ), counterbalancing the decreases in μ and leading to improvements in L and hence higher cell efficiencies.

This study is undertaken by combining numerical simulations and experimental data obtained from the electrical characterizations of SoG-Si, purified by the metallurgical route, wafers and solar cells

2 EFFECTS OF COMPENSATION ON CARRIER LIFETIME

2.1 Case of doping species

Doping species, such as boron (B), phosphorus (P), aluminium (Al), introduce energy levels in the silicon band gap in the vicinity of the valence band (E_v) for acceptor species (B, Al) or in the vicinity of the conduction band (E_c) for donor species (P). These energy levels are known to enhance the trapping of the free carriers, but present at high levels they can also contribute significantly to carrier recombination. By applying Shockley-Read-Hall (SRH) statistic [3], it is possible to compute the effects of doping species on τ. For instance, B introduces in the silicon band gap an energy level located at 0.045 eV above E_v. Due to the proximity of this energy level with E_v, the carrier recombination rate is limited by the capture of electrons by the neutral dopant. The electron capture cross section (σ_n) of neutral B has not been determined accurately and values from the literature concerning capture cross sections of various neutral dopants cover several orders of magnitude [2]. In our simulations, σ_n was thus allowed to vary from 10^{-17} cm^2 to 10^{-19} cm^2, 10^{-17} cm^2 being, as proposed by Geerligs et al. [2], a likely upper bound for a neutral dopant capture cross section.

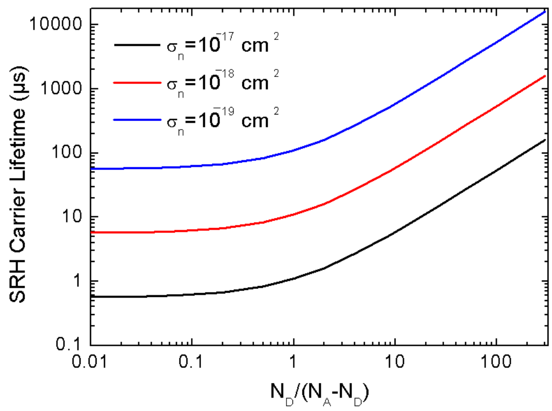

Figure 1: Evolution with C_l of τ limited by recombination throughout B atoms in *p*-type silicon, computed from SRH statistic. Comparison between different values for the electron capture cross-section of neutral B.

Fig. 1 presents the evolution of τ, due to the effects of B atoms, with the compensation level (C_l), computed from the SRH statistic. C_l is defined as $N_D/(N_A-N_D)$, N_A and N_D being respectively the total concentrations of acceptor and donor species. Notice that for this simulation, we considered only *p*-type silicon ($N_A > N_D$), fixed [B] equal to 3×10^{17} cm^{-3} and took the injection level (Δn) equal to 10^{12} cm^{-3}, which corresponds to low-injection conditions. We checked that the simulation results were only weakly dependent on Δn, at least as long as Δn remains much smaller than N_A. Only B is present as acceptor element, consequently N_A=[B]. Fig. 1 shows a drastic increase of τ with C_l. Indeed when C_l varies from 0.1 to 10, τ is multiplied by 10. This means that increase in C_l reduces considerably the recombination strength of B atoms and could lead to strong improvements in the efficiency of highly B doped solar cells. To account for this a priori surprising result, let us first consider the comparison with standard uncompensated *p*-type silicon. When the doping level is increased, the recombination strength of shallow levels is expected to increase. Indeed, the Fermi level (E_F) gets closer to the acceptor energy level, and by modifying its charge state, enhances its ability for the capture of minority carriers. Thus, in such a strongly doped *p*-type material, the reduction of the free carrier concentration through the increase of the concentration of donors results in a shift of E_F towards the center of the gap, meaning that the attractivity of neutral B atoms for electrons is reduced, and resulting in an increase of τ. In this first set of simulations, we neglected possible interactions between B and donor or metallic species. We also used the simplified SRH statistic, instead of the more general solution of the continuity equations that takes into account carrier trapping. The recombination centers density being very high (3×10^{17} cm^{-3}), we used a model by Macdonald and Cuevas [4] to check whether this simplified SRH statistic could be applied. The Macdonald and Cuevas model states that the simplified SRH statistic can only be applied if the recombination center density is at least one order of magnitude lower than a critical level N_{crit} which depends on the location of the energy level in the silicon band gap, on the ratio (κ) between the hole and electron capture cross sections, and on the hole concentration (p_0). In our simulations with low-injection conditions, the lowest value of N_{crit} is obtained for the lowest p_0 value (10^{15} cm^{-3}) and the lowest κ value. The hole capture cross section (σ_p) of ionized B^- is generally assumed, due to a strong Coulombic attraction, to be very large. For instance a value for σ_p of 7.65×10^{-12} cm^{-2} measured at 4.2 K is reported in Ref. 5. Thus a κ value equal to 10 can be seen as a very safe lower bound for κ. However, even with κ=10, we found that the minimum value for N_{crit} (in low-injection condition) was equal to 5.2×10^{18} cm^{-3}. Such a large value can be traced to the proximity of the B energy level to E_v [4]. In any case, the conclusion is that the use of the simplified SRH model in our simulations was fully justified.

2.2 Case of metal impurities

SoG Si contains high concentrations of doping species, but also large concentrations of metal-impurities (especially iron Fe and chromium Cr). In a second set of simulations, we showed that an increase in C_l reduces also the recombination strength of metal-impurities. Interstitial metal impurities (Fe, Cr) are in thermal equilibrium generally paired with substitutional B atoms. These donor acceptor pairs introduce, like doping species, shallow energy levels in the silicon band gap. For instance the iron-boron (FeB) pair introduces an energy level located at 0.26 eV below E_c and the chromium-boron (CrB) pair introduces an energy level located at 0.28 eV above E_v [6,7] σ_n and σ_p of both pairs have been determined at 300 K [8,9]. We computed, from SRH statistic, the variation of τ limited by these complexes with C_l, as shown in Fig. 2. In these simulations, [B] and Δn are respectively set to 10^{16} and 10^{12} cm^{-3}. As shown in Fig. 2, due again to the shift of E_F towards mid-gap, τ increases strongly with C_l (for Fe, when C_l varies from 0.1 to 10, τ is multiplied by about 3). In other words, an increase in C_l reduces the recombination strength of both FeB and CrB pairs and limits their effect on solar cell performance. An important issue to be discussed is that donor-acceptor pairs are formed only if Coulomb attraction is present. If E_F is shifted above the energy level introduced by the donor state of the metallic impurity, the interstitial atom is in its neutral state and the pair cannot be formed [10]. Regarding interstitial Cr, its donor level is located at E_c-0.22 eV [7].

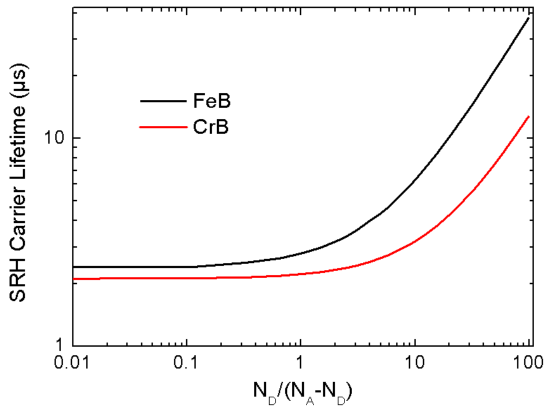

Figure 2: Evolution with C_l of τ limited by recombination throughout FeB and CrB pairs in *p*-type silicon, computed from SRH statistic.

Since our focus is only on *p*-type Si, E_F remains always in the lower half of the Si band gap and therefore the CrB pair is formed even at high C_l. As for interstitial Fe, its donor level is located at E_v+0.38 eV [6], also in the lower half of the gap, therefore the situation is a priori more complex. However, even at the highest C_l considered in our simulations, p_0 remains above 10^{14} cm^{-3}. The E_F corresponding to this value is located at E_v+0.3 eV, *i.e.* below the level introduced by Fe_i. As a consequence, it can also be safely assumed that FeB pairs remain associated even at high C_l.

2.3 Auger and radiative recombinations

By reducing p_0, increases in C_l reduce also the Auger and radiative recombination rates, which both, especially for low-injection conditions, increase strongly with the free carrier concentration [11]

2.4. Application for highly-doped silicon solar cells

In Fig. 3 we computed via the simulation software PC1D [12] the variation of the conversion efficiency (η) of a highly B-doped solar cell with the P concentration. For this simulation, σ_n for the B atoms is equal to 7×10^{-18} cm^{-3}. We neglected recombination throughout P atoms. Nevertheless, Auger recombination is taken into account. Effects of both doping species on μ is taken into account by using the empiric expression linking μ for electrons and holes with the sum [P]+[B] given in Ref. 13.

These simulation results confirm that increases in C_l, reduce the recombination strength of the B atoms and can lead to strong improvements in η. For instance, for $[B]=6\times10^{17}$ cm^{-3}, when [P] varies from 10^{16} cm^{-3} to 4×10^{17} cm^{-3}, η varies from 10.5% to 12.2% (1.7 absolute %). This reveals the high potential of an accurate control of C_l to increase the efficiency of highly doped silicon solar cells.

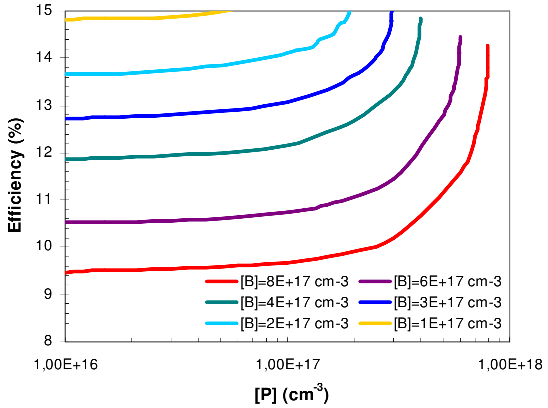

Figure 3: Computed variation of the conversion efficiency of a highly B-doped solar cell with the P concentration.

3.3 Experimental verification

To experimentally confirm this theoretical study, a multicrystalline silicon (*mc*-Si) ingot was grown from a highly compensated Si feedstock purified by the metallurgical route [14]. B and P feedstock concentrations, estimated from Glow-Discharge-Mass-Spectroscopy (GDMS) measurements, were respectively equal to 3.1×10^{17} cm^{-3} and 3.4×10^{17} cm^{-3}. With such a feedstock material, the difference in partition coefficients (k) between P (k = 0.35) and B (k = 0.8) induced a change in the type of conductivity (*p*- to *n*-type Si) from the bottom to the top of the ingot [15]. A wafer from the bottom part of this ingot was electrically characterized in terms of resistivity (ρ), as shown in Fig. 3. ρ was measured by the eddy current method. The ρ map reveals a strong increase of ρ from the edges to the center of the wafer. We measured by GDMS [B] and [P] on the edges and at the centre of the wafer. On the edges, [B] was equal to 2.6×10^{17} cm^{-3} and [P] equal to 1.4×10^{17} cm^{-3}. Around the center, [B] remained equal to 2.6×10^{17} cm^{-3} but [P] was up to 2.1×10^{17} cm^{-3}. For a dopant such as P with a relatively small partition coefficient, convecto-diffusive solute transport in molten silicon, along with the curvature of the crystallization front, induce a significant increase of [P] from the edges to the center of the wafers. On the other hand, the partition coefficient of B being much closer to unity, these factors have only a very limited influence on the repartition of B across the wafer. Therefore, C_l increases from the edges to the centre of the wafer (from 1.2 to 4.2).

Knowing the hole concentration ([B]-[P]) and ρ values, we estimated the hole mobility (μ_p) on the edges and on the center of the wafer by the formula $\rho\ \mu_p$ ([B]-[P]) |e| = 1. On the edges μ_p was equal to 110 $cm^2.V^{-1}.s^{-1}$ and on the center equal to 50 $cm^2.V^{-1}.s^{-1}$. Such values call for two comments : first, they are quite low on an absolute scale, meaning that they are in our SoG material many scattering centers, not only dopants but also metallic impurities. As for the difference in μ_p between center and edges of the wafer, it should be kept in mind that these metallic impurities, dissolved and/or precipitated will like P segregate around the center, and their effect on mobility is thus expected to be stronger there. A point that should be stressed is that the crystallographic characteristics (dislocation density, grain size) were very homogeneous on the surface of the wafer.

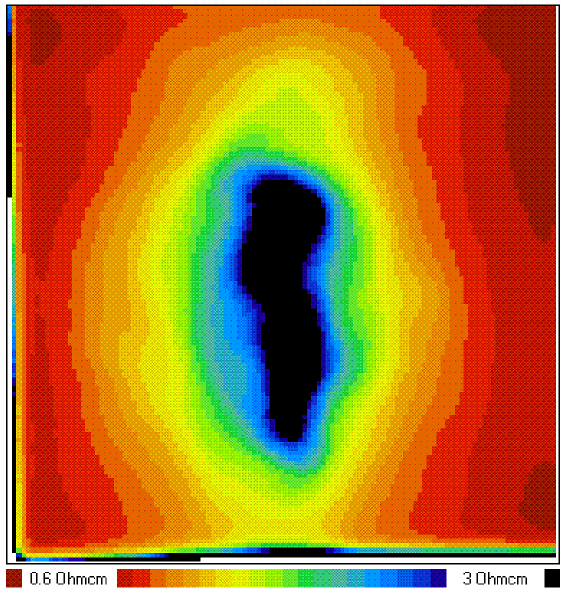

Figure 3: Resistivity map of a mc-Si wafer from an ingot grown from a strongly compensated silicon feedstock purified via a metallurgical process.

From this wafer, a solar cell was made by using a standard industrial process at the RESTAURE platform at CEA-INES [16]. Then, a light beam induced current (LBIC) map was made at various near infrared wavelengths, which enabled us to compute a L map, as shown in Fig. 4. The formula $L=(D\tau)^{0.5}$, where D stands for the electron diffusion coefficient, allows to identify two competing mechanisms: similarly to what has been observed for holes, we can legitimately suppose that the electron mobility (μ_e) is also affected by increases in the total amount of impurities. As D is directly proportional to μ_e, a negative contribution can be expected. Nevertheless, we can observe a strong increase of L, from 75 μm to 147 μm from the edges to the center of the wafer. This increase is perfectly correlated with the increase of C_l, and confirms that the strong increase in τ with C_l counterbalances the effect of the increase of the total amount of impurities on μ, and thus leads to increase in L. Even without considering the effect of the variation of mobilities, this means that τ is at least multiplied by 3.8 when C_l varies from 1.2 to 4.2.

Table 1: Compensation level, hole mobility and minority carrier diffusion length of the SoG-Si solar cell. Values determined at the center and on the edges of the cell.

	Cl	μ_p ($cm^2.V^{-1}.s^{-1}$)	L_n (μm)
Edge	1.2	110	75
Center	4.2	50	147

By comparing this result with the previous simulations, this very strong dependence of τ with C_l means probably that in the finished cell τ is rather limited by doping species than metal impurities, which have been probably removed by the efficient gettering effect developed by the P-diffusion (to form the emitter) [17].

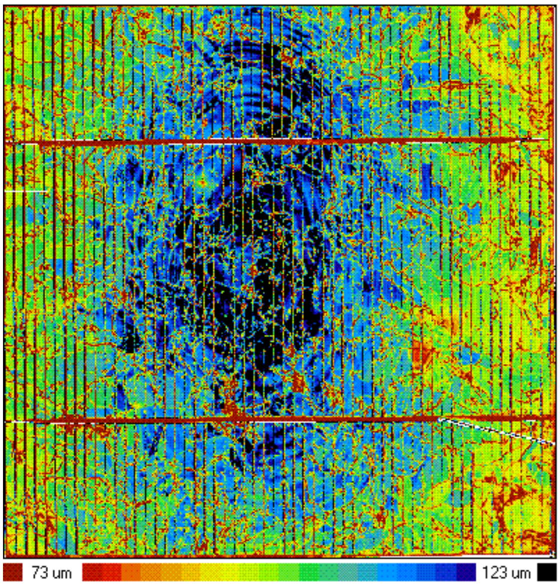

Figure 4: Figure 4: Minority carrier diffusion length map of a mc-Si solar cell from an ingot grown from a strongly compensated silicon feedstock purified via a metallurgical process.

4 LIMITS OF COMPENSATION ON SOLAR CELL PERFORMANCES

Increases in C_l improve τ. Consequently, we can legitimately suppose that increases in C_l will also improve the efficiency of Si solar cells containing a large amount of impurities. Nevertheless we will show that increases in C_l have also their limits concerning the cells performances.

First, increases in C_l affect both the electron and hole mobility. Thus very high C_l may affect both the J_{cc} (by affecting L_n) and the Fill Factor (by increasing the series resistances) of the cell.

In addition, when C_l is very high, due to the location of E_F towards the center of the Si band gap, the band curvature is lower, and consequently low Open Circuit V_{oc} are expected to be found.

Third, high C_l being associated with large amounts of doping species, numerous interactions between doping species themselves, or between doping species and other elements (metal impurities, carbon, oxygen, as shown in Ref. 18) may also affect τ and counterbalance the beneficial effects of the compensation.

Finally, it's particularly difficult to accurately control C_l. One possibility is to add to the feedstock a given concentration of B or P. Nevertheless, due to the stronger segregation of P compared to B, C_l will strongly vary on the ingot length and in addition changes in the type of conductivity may occur. Variation of C_l on the surface of the wafer, especially if the front of crystallisation is disturbed, may also occur.

5 CONCLUSION

Our purpose in this letter was to demonstrate that compensation can induce strong improvements in τ values. Chemical and electrical characterizations of strongly compensated *mc*-Si wafers and solar cells, which show a strong correlation between increases in C_l and L, support the theoretical findings. These results are of paramount importance, since an accurate control of C_l throughout the feedstock selection, the ingot crystallisation, or in the as-cut wafer, can lead to strong improvements in both τ and cell efficiencies.

AKNOWLEGMENTS

The authors would like to thank FerroPem company for the supply of metallurgically purified Si feedstock, and the Apollon Solar and Cyberstar companies for the crystallization of the feedstock material.

REFERENCES

[1] M. Cuevas, Physical Review. 164, 1021 (1967).
[2] L. J. Geerligs, D. Macdonald and G. Coletti, 17th NREL Workshop on Crystalline Silicon Solar Cells & Modules: Materials and Processes, Vail, Colorado, 5-8 August, 2007.
[3] W. Shockley and W. T. Read, Phys. Rev. 87, 835 (1952).
[4] D. Macdonald and A. Cuevas, Physical Review B. 67, 075203 (2003).
[5] J. M. Brown and A. J. Jordan, J. Appl. Phys. 37, 337 (1966).
[6] A. A. Istratov, H. Hieslmair, E. R. Weber, Appl. Phys. A 69, 13-44 (1999).
[7] H. Conzelmann, K. Graff and E. R. Weber, Appl. Phys. A 30, 169 (1983).
[8] D. Macdonald, T. Roth, P. N. K. Deenapanray, T. Trupke and R. A. Bardos, Appl. Phys. Lett. 83, 142107 (2006).
[9] J. Schmidt, R. Krain, K. Bothe, G. Pensl and S. Beljakova, J. Appl. Phys. 102, 123701 (2007).
[10] E. R. Weber, Appl. Phys. A: Solids Surf. 30, 1 (1983).
[11] D. K. Schroder, IEEE Transactions on Electron Devices. 44, 160 (1997).
[12] P. A Basore, Proceedings of the 22nd IEEE Photovoltaic Specialists Conference, 299 (1991).
[13] N. D. Arora, J. R. Hauser and D. J. Roulston, IEEE Trans. Electron Devices 29. 292 (1982).
[14] R. Einhaus, Y. Caratini, D. Bernou, F. Servant, R. Monna, C. Trassy, J. Kraiem, J. Degoulange, S. Martinuzzi, I. Périchaud, Proc. of the 21st EPVSEC, Dresden, Germany (2006).
[15] R. Einhaus, J. Kraiem, F. Lissalde, S. Dubois, N. Enjalbert, R. Monna, To be published in the Proceedings of the 33rd IEEE Photovoltaic Specialists Conference, San Diego (IEEE, New York, 2008).
[16] R. Monna, J. F. Lelièvre, M. Pirot, S. Noel, N. Rondel, M. Lemiti and C. Jaussaud, Proceedings of the 20th European Photovoltaic Solar Energy Conference, Barcelona, Spain (WIP, Munich, 2005), p. 1152.
[17] S. Dubois, O. Palais, P. J. Ribeyron, N. Enjalbert, M. Pasquinelli and S. Martinuzzi, J. Appl. Phys. 102, 083525 (2007).
[18] S. Dubois, N. Enjalbert, J. P. Garandet, R. Monna, J. Kraiem, in the proceedings of this conference.